Journal of Engineering Mathematics **42:** 373–388, 2002.

Deep- and shallow-water slamming at small and zero deadrise angles

S. D. HOWISON, J. R. OCKENDON and J. M. OLIVER
OCIAM, Mathematical Institute, 24–29 St Giles, Oxford OX1 3LB, U.K.; e-mail: howison@maths.ox.ac.uk

Received 27 November 2001; accepted in revised form 30 January 2002

Abstract. This paper reviews and extends theories for two classes of slamming flows resulting from the violent impact of bodies on half-spaces of inviscid fluid. The two configurations described are the impact of smooth convex bodies, and of non-smooth but flat-bottomed bodies, respectively. In each case, theories are presented first for small penetration depths in finite- or infinite-depth fluids (which we call Wagner flows), and secondly when the penetration is comparable to the fluid depth (which we call Korobkin flows). We also discuss the transition from Wagner flow to Korobkin flow.

Key words: free-surface flow, inviscid hydrodynamics, ship slamming, water entry

1. Introduction

This paper is concerned with two theories of two-dimensional, high-velocity impact between a rigid body and the initially planar boundary of an inviscid fluid. Motivated by naval architecture, we refer to such problems as slamming problems. Our aim is to review and unify the two theories, and also to present some new results.

The first theory is the classical one of Wagner [1], in which the fluid initially occupies a half-space $y < 0$ and the impacting body is two-dimensional, convex and nearly tangential to the x-axis. This situation is called that of 'small deadrise angle' in naval architecture and it produces higher dynamic pressures than does an impactor with any other geometry. We will denote the order of magnitude of the deadrise angle between the impactor and the x-axis by ϵ. The key observation in [1] is that the motion generated in the liquid is almost the same as that produced by a flat plate that lies approximately along the x-axis, and moves into $y < 0$ with speed V, but expands its length at a rate $O(V/\epsilon)$.

The 'effective plate' corresponds to that part of the wetted area between the thin 'splash jets' indicated in Figure 1, and its length is found by solving a 'codimension-two free-boundary problem' [2]. Indeed, this free-boundary problem is so simple that it can be solved explicitly for arbitrary convex, small-deadrise impactors. Moreover, as shown in [2], the systematic

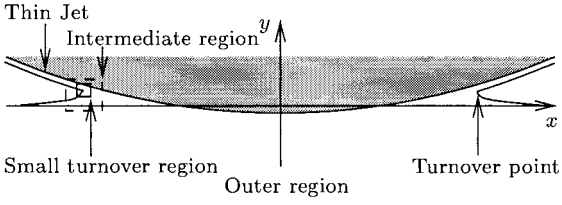

Figure 1. Structure of small deadrise angle impact in the Wagner limit of small penetration.

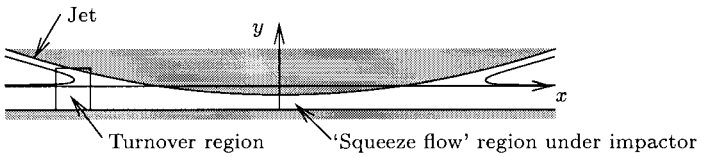

Figure 2. Structure of small deadrise angle impact in the Korobkin flow regime.

asymptotic description of this theory involves separate analyses in the bulk of the liquid, in the 'turnover' region near the root of the splash jet and in the splash jet itself (we shall also see that there is an intermediate region between the outer region and the root of the splash jet, but the solution there turns out to be trivial). The relative sizes of these regions will be made precise in the following section.

The Wagner theory can be extended to liquids of constant finite depth, provided that the liquid depth is of $O(\epsilon)$ relative to the radius of curvature of the impactor and the penetration is small compared with that depth; this is a relatively straightforward exercise in conformal mapping. However, when the penetration is no longer small relative to the depth, a new theory becomes necessary. This fact was pointed out and resolved by Korobkin [3] who realised that for penetrations of the same order as the liquid depth, the flow has to be decomposed into three quite different regions for the purpose of a matched asymptotic analysis. These regions are indicated in Figure 2; the fact that the regions near the ends of the 'equivalent plate' now extend from the impactor to the base of the liquid means that we are now confronted with a full 'codimension-one' free boundary problem for the flow directly beneath these parts of the impactor.

Our first objective in this paper is to reconcile the Wagner and Korobkin theories and we do this in Section 3, where we also point out the analogy between the turnover flow in Figure 2 and the theory of skimming proposed in [4].

Our second objective is to make some preliminary observations about slamming when the impactor has zero deadrise angle over a segment and finite deadrise angle elsewhere as in Figure 7(a). In particular, in Section 4, we consider the normal impact of a rectangle under the assumption that the flow separates smoothly from its corners as in Figure 8(b). When the liquid has infinite depth, the 'outer' solution away from the corners corresponds to a Wagner flow in which the equivalent plate is prescribed and equal to the base of the cylinder (see [5, Chapter 6]). However, the local solution near the corners poses a much more difficult problem than does the solution in the splash root of Figure 1, with repercussions when we again try to reconcile the infinite depth flow with the shallow water impact theory of [6]. The latter theory, which agrees well with the experiments of [7], leads to another codimension-one free boundary problem in which the free boundary now corresponds to the spout of water depicted in Figure 10 of that paper. Finally, in Section 5 we will consider some new results on three-dimensional Wagner and Korobkin flows, and also cite some of the many open problems that these solutions pose.

2. The Wagner theory

We start by considering impact into water of finite depth H, in which the scenario for the Wagner theory is that of Figure 1 but with a base at this depth. We suppose that the impactor has radius of curvature of $O(H/\epsilon)$, where $\epsilon \ll 1$, and is moving downwards with speed V. Because the impactor is blunt, the effects of finite depth are felt before it has penetrated

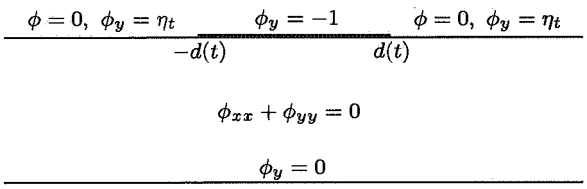

Figure 3. Leading order outer Wagner problem. The conditions at $t = 0$ are $\phi = 0$, $\eta = 0$, and $\phi \to 0$ as $x \to \pm\infty$. The conditions at $x = \pm d(t)$ are stated in the text. Suffices denote partial derivatives.

far into the water, and they become important when the lateral extent of the portion of the impactor below the undisturbed water surface is of $O(H)$, which in general occurs for times of $O(\epsilon H/V)$. We thus take dimensionless coordinates x and y scaled with H, and time t scaled with $\epsilon H/V$. The motion is irrotational and we denote the velocity potential, scaled with VH, by $\phi(x, y, t)$. We denote the surface elevation, which may be multi-valued, by $y = \epsilon\eta(x, t)$ and the impactor body by $y = \epsilon\,(f(x) - t)$, with $f(0) = 0$. We could assume that $f(x)$ is an arbitrary smooth convex function but, for simplicity, we only consider $f(x) = x^2$ until we deal with flat-bottomed impactors.[1]

As proposed by Wagner [1] and explained in detail in [8], the free surface is confined to the region $|x| > d(t)$, where $d(t) = O(1)$ as $\epsilon \to 0$. The points where $|x| = d(t)$ define points of vertical tangency between a lower segment of the free surface, which is displaced by $O(\epsilon)$ from the x-axis, and an upper segment which delineates the splash jet shown in Figure 1. We refer to the vicinity of one of these points as a turnover region.

Away from the turnover regions, as $\epsilon \to 0$ the 'outer' problem for ϕ and η can be written as a mixed boundary-value problem in the strip $-\infty < x < \infty$, $-1 < y < 0$. The flow in the splash jet is ignored and, under the additional assumption that the flow starts from rest and remains at rest at infinity (see [9] for a justification of this assumption), the full free boundary conditions

$$\frac{\partial\phi}{\partial y} = \frac{\partial\eta}{\partial t} + \epsilon\frac{\partial\phi}{\partial x}\frac{\partial\eta}{\partial x}, \qquad \frac{\partial\phi}{\partial t} + \frac{1}{2}\epsilon\,|\nabla\phi|^2 = 0$$

on $y = \epsilon\eta(x, t)$ reduce to

$$\frac{\partial\phi}{\partial y} = \frac{\partial\eta}{\partial t}, \qquad \phi = 0 \quad \text{on } y = 0,\ |x| > d(t), \tag{1}$$

$$\frac{\partial\phi}{\partial y} = -1 \qquad\qquad \text{on } y = 0,\ |x| < d(t). \tag{2}$$

This 'linearisation' of Figure 1 is depicted in Figure 3.

As shown in [9], writing $z = x + \mathrm{i}y$, the complex potential $w(z, t)$ satisfies

$$\frac{\partial w}{\partial z} = \frac{\pi}{Q\,(\zeta, b(t))}\int_0^1 Q\,(s, b(t))\left(\frac{1}{s + c(t)} - \frac{1}{s - \zeta}\right)\mathrm{d}s, \tag{6}$$

where

$$\zeta(z, t) = \frac{\mathrm{e}^{\pi z} - \mathrm{e}^{-\pi d(t)}}{\mathrm{e}^{\pi d(t)} - \mathrm{e}^{-\pi d(t)}}, \qquad Q(\zeta, b) = \left(\frac{\zeta(1 - \zeta)}{\zeta + b}\right)^{\frac{1}{2}},$$

[1] In [8], the body was described by writing it as $y = f(\epsilon x) - t$ which, by a redefinition of the coordinates, can be written as our $y = \epsilon\,(f(x) - t)$; thus care may be needed in comparing the two.

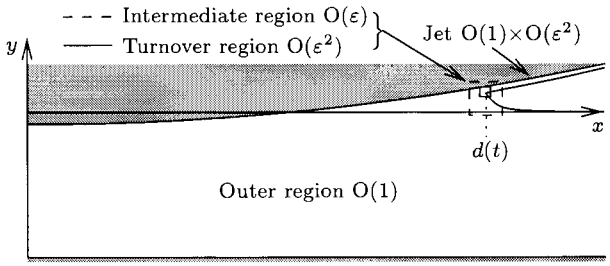

Figure 4. Structure of small deadrise angle impact into a finite-depth layer of fluid.

and

$$b(t) = \frac{1}{\mathrm{e}^{2\pi d(t)} - 1}, \qquad c(t) = \frac{1}{\mathrm{e}^{\pi d(t)} - 1};$$

the square roots are chosen appropriately and the integral is taken along the real s-axis. This result can be expressed in terms of elliptic integrals but its most important consequence is that, as $z \to d(t)$,

$$w(z,t) \sim -\left(\frac{2\mathrm{i}}{\pi^{\frac{3}{2}}}(1+c(t))\int_0^1 \frac{s^{\frac{1}{2}}\,\mathrm{d}s}{(s+b)^{\frac{1}{2}}(1-s)^{\frac{1}{2}}(s+c(t))}\right)(z-d(t))^{\frac{1}{2}}. \tag{4}$$

Also w decays exponentially as $|z| \to \infty$ (this decay is only algebraic when $H = \infty$). We remark that the complexity of (3) means that, in practice, for many slamming problems it is easiest to proceed numerically by direct discretisation of the variational formulation introduced by [10] (see, for example, [8]).

In order to determine $d(t)$, and thereby close the problem, we need to consider the behaviour near $z = d(t)$ more closely. As elucidated in [8], the singularity in (4) can be removed by matching with a turnover region in which $y - \epsilon\left(d^2(t) - t\right) = O(\epsilon^2)$, $x - d(t) = O(\epsilon^2)$. The situation is as sketched in Figure 4, which also indicates that the matching should strictly be performed through an intermediate region in which $y = O(\epsilon)$, $x - d(t) = O(\epsilon)$. However, it is soon apparent that in this intermediate region the solution is, to lowest order, simply the local form near $z = d(t)$ of the solution of the outer mixed boundary value problem of Figure 3, given by (4). The key point is that $x = d(t)$, which is the point of vertical tangency of the free surface, is located at a distance of $O(\epsilon^2)$ from the impactor, which implies that the free surface, as given in the outer solution from (1) by

$$\eta(x,t) = \int_0^t \frac{\partial\phi}{\partial y}(x,0,\tau)\,\mathrm{d}\tau,$$

must satisfy

$$\eta\big(d(t),t\big) = d^2(t) - t. \tag{5}$$

Of course, this can only be justified by constructing the solution in the turnover region and, as shown in [8], this is done by solving a simple Helmholtz free boundary flow in a frame moving with the turnover point. This calculation also reveals that all the fluid that feeds the splash jets originates from the region $|x| > d(t)$; to this order, no fluid is squeezed out from under the body into the jet.

The consequence of (5) is that $d(t)$ satisfies

$$d^2(t) - t = \frac{1}{\pi}\int_0^t \frac{(\zeta(d(t),\tau)+b(\tau))^{\frac{1}{2}}}{\zeta(d(t),\tau)^{\frac{1}{2}}\,(\zeta(d(t)t,\tau)-1)^{\frac{1}{2}}} \times \int_0^1 \frac{s^{\frac{1}{2}}(1-s)^{\frac{1}{2}}}{(s+b(\tau))^{\frac{1}{2}}}\left(\frac{1}{s+c(\tau)} - \frac{1}{s-\zeta(d(t),\tau)}\right) \mathrm{d}s\ \mathrm{d}\tau. \tag{6}$$

An interesting physical consequence of this asymptotic solution is that the leading order outer pressure, as given by

$$\left.\frac{\partial\phi}{\partial t}\right|_{y=0,|x|>d(t)},$$

is $O\left(\epsilon^{-1}\right)$ relative to ρV^2, but has a square root singularity as the intermediate regions $|x \mp d(t)| = O(\epsilon)$ are approached. This makes the pressure in these regions of $O\left(\epsilon^{-\frac{3}{2}}\right)$, while in the turnover regions, where $x \mp d(t) = O(\epsilon^2)$, it is $O(\epsilon^{-2})$. Hence the outer region contributes $O\left(\epsilon^{-1}\rho V^2 H\right)$ to the force per unit length on the impactor, and dominates the $O\left(\epsilon^{-\frac{1}{2}}\rho V^2 H\right)$ contribution from the intermediate regions, which in turn dominates the $O\left((\rho V^2 H\right)$ contribution from the turnover regions.

3. The Korobkin theory

For the purposes of this paper, the most important deduction from (4), (5) is the large-time behaviour of the solution. While it is easy to show from (5) that $d(t) \sim (2t)^{\frac{1}{2}}$ as $t \to 0$, it is less apparent that $d(t) \sim (3t)^{\frac{1}{2}}$ as $t \to \infty$. However, this result, which can be derived as the large-time limit of (6), will also emerge on the small-time limit of the next step in the evolution of the slamming, namely the scenario proposed by Korobkin in [3] and shown in Figure 2. We consider a rescaling of the variables used hitherto, writing

$$t = T/\epsilon, \quad x = X/\epsilon^{\frac{1}{2}}, \quad d(t) = D(T)/\epsilon^{\frac{1}{2}}, \quad \phi(x,y,t) = \Phi(X,y,T).$$

In this regime the impactor has penetrated to a depth of $O(H)$, and the problem away from the turnover region and the splash jet is

$$\epsilon\frac{\partial^2\Phi}{\partial^2 X} + \frac{\partial^2\Phi}{\partial^2 y} = 0 \quad \text{with} \quad \frac{\partial\Phi}{\partial y} = 0 \quad \text{on } y = -1, \tag{7}$$

together with conditions on the impactor and the free surface. In the region $|X| < D(T)$, the impactor is now $y = X^2 - T$ $(0 < T < 1)$, on which we have

$$\frac{\partial\Phi}{\partial y} = -1 + 2\epsilon X\frac{\partial\Phi}{\partial X}. \tag{8}$$

For $|X| > D(T)$, however, the free surface may now suffer a much larger displacement from its original position, and we write it as $y = h(X,T)$; the free boundary conditions are then

$$\frac{\partial\Phi}{\partial y} = \frac{\partial h}{\partial T} + \epsilon\frac{\partial\Phi}{\partial X}\frac{\partial h}{\partial X}, \quad \frac{\partial\Phi}{\partial T} + \frac{1}{2}\left(\left(\frac{\partial\Phi}{\partial y}\right)^2 + \epsilon\left(\frac{\partial\Phi}{\partial X}\right)^2\right) = 0$$

on $y = h(X, T)$. As usual we require $\Phi \to 0$ as $|X| \to \infty$ but the initial conditions need further discussion, as does the solution in the turnover region. Let us first, however, consider the implications of (7), (8).

The high velocities generated under the impactor, together with (7), suggest that Φ has an expansion in the form

$$\Phi(X, y, T) \sim \frac{1}{\epsilon}\Phi_0(X, T) + \Phi_1(X, y, T) + \cdots,$$

where the solvability condition for Φ_1 implies that

$$\left(1 + X^2 - T\right)\frac{\partial \Phi_0}{\partial X} = 1 - 2X\frac{\partial \Phi_0}{\partial X}, \tag{9}$$

yielding the mass conservation statement that

$$\frac{\partial \Phi_0}{\partial X} = \frac{X}{1 + X^2 - T}. \tag{10}$$

We note that the corresponding pressure is

$$-\frac{1}{\epsilon}\left(\frac{\partial \Phi_0}{\partial T} + \frac{1}{2}\left(\frac{\partial \Phi_0}{\partial X}\right)^2\right),$$

but we do not yet know its value as we approach the turnover region near $X = D(T)$. The only scaling that can reinstate the nonlinear free boundary condition near the turnover region is to write

$$D(T) \sim D_0(T) + O(\epsilon), \qquad X - D_0(T) = \epsilon^{\frac{1}{2}}\xi$$

with the corresponding potential

$$\epsilon^{-\frac{1}{2}}\left(\dot{D}_0\xi + \varphi(\xi, y, T)\right). \tag{11}$$

This gives, to lowest order,

$$\frac{\partial \varphi}{\partial \xi} + \frac{\partial \varphi}{\partial y} = 0 \quad \text{with} \quad \frac{\partial \varphi}{\partial y} = 0 \quad \text{on } y = -1\,.$$

On the body, $y = D_0^2 - T$, to lowest order we have $\partial\varphi/\partial y = 0$, and on the free surface $y = h(X, T) = H(\xi, T)$

$$\frac{\partial \varphi}{\partial y} - \frac{\partial \varphi}{\partial \xi}\frac{\partial H}{\partial \xi} = \epsilon^{\frac{1}{2}}\frac{\partial H}{\partial T},$$

$$\left(\frac{\partial \varphi}{\partial \xi}\right)^2 + \left(\frac{\partial \varphi}{\partial y}\right)^2 - \dot{D}_0^2 = -2\epsilon^{\frac{1}{2}}\left(\ddot{D}_0\xi + \frac{\partial \varphi}{\partial T}\right). \tag{12}$$

Hence, to lowest order in the turnover region we have another Helmholtz flow in which T enters only as a parameter (see Figure 5). This is in fact the 'skimmer' flow analysed in [4], where an explicit solution is presented that satisfies the boundary conditions

$$\varphi \sim -V_1\xi \quad \text{as} \quad \xi \to -\infty,\ -1 < y < D_0^2 - T \quad \text{(under the impactor)}, \tag{13}$$

$$\varphi \sim V_2\xi \quad \text{as} \quad \xi \to \infty,\ H_\infty < y < D_0^2 - T \quad \text{(the splash jet)}, \tag{14}$$

$$\varphi \sim -V_2\xi \quad \text{as} \quad \xi \to \infty,\ -1 < y < 0 \quad \text{(the undisturbed fluid)}. \tag{15}$$

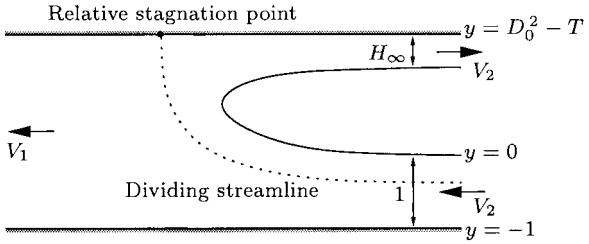

Figure 5. Turnover region for a Korobkin flow.

This solution reveals that, for these Korobkin flows, all the fluid in the (now very strong) jet still emanates from the undisturbed region ahead of the jet (in which the fluid velocities are exponentially small as $\epsilon \to 0$), rather than from under the body. However, (15) is only consistent with an undisturbed fluid region far ahead of the turnover region, and (14), (15) are only consistent with the lowest-order Bernoulli condition (12) there, if $V_2 = \dot{D}_0$.

It remains to determine D_0, H_∞ and V_1. The obvious velocity matching between (7) and (13) requires that

$$-V_1 + \dot{D}_0 = \frac{D_0}{1 + D_0^2 - T},$$

and an obvious mass conservation condition for (13)–(15) is

$$V_1\left(1 + D_0^2 - T\right) = V_2 - V_2\left(D_0^2 - T - H_\infty\right).$$

This last condition is a trivial consequence of

$$\iint_{\text{flow domain } \Omega} \nabla^2\varphi \, \mathrm{d}S = \int_{\partial\Omega} \frac{\partial\varphi}{\partial n} \, \mathrm{d}s,$$

but the further identity for a harmonic function φ that

$$\int_{\partial\Omega} \frac{1}{2} |\nabla\varphi|^2 \mathbf{n} \, \mathrm{d}s = \int_{\partial\Omega} \frac{\partial\varphi}{\partial n} \nabla\varphi \, \mathrm{d}s,$$

which can be shown to be equivalent to conservation of momentum, leads to

$$\tfrac{1}{2}V_1^2\left(1 + D_0^2 - T\right) + \tfrac{1}{2}V_2^2\left(1 + D_0^2 - T\right) = V_2^2\left(1 + H_\infty\right).$$

Remembering that $V_2 = \dot{D}_0$, we finally obtain the law of motion of the turnover region as

$$\dot{D}_0 = \frac{D_0}{2\left(1 + D_0^2 - T\right)} \left(1 - \left(1 + D_0^2 - T\right)^{-\frac{1}{2}}\right)^{-1}. \tag{16}$$

For future reference, we note that, from (10),

$$\left.\frac{\partial\Phi_0}{\partial X}\right|_{X=D_0} = 2\dot{D}_0\left(1 - (1 + D_0^2 - T)^{\frac{1}{2}}\right); \tag{17}$$

also, since $\varphi \sim -V_1\xi$ as $\xi \to -\infty$, matching of (11) with the solution of (9) shows that

$$\Phi_0 \to 0 \qquad \text{as} \quad X \to D_0(T), \tag{18}$$

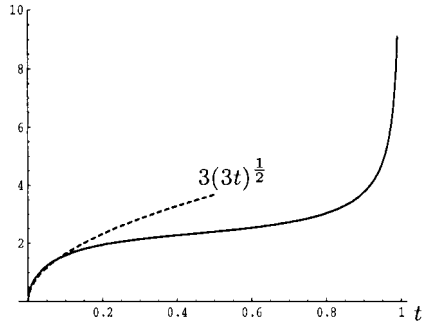

Figure 6. Dimensionless force per unit length in a Korobkin flow.

which amounts to saying that to leading order the potential does not jump across the turnover region. It can also be shown that, relative to ρV^2, the pressure in the turnover region varies from

$$\frac{1}{\epsilon^{\frac{3}{2}}}\left(\frac{2\dot{D}_0^2}{1+D_0^2-T}\left(\left(1+D_0^2-T\right)^{\frac{1}{2}}-1\right)\right)$$

to zero as ξ goes from $-\infty$ to ∞. Hence, as in the Wagner theory, the leading-order body force comes from the region $0 < X < D(T)$, and is of $O(\epsilon^{-2})$. Following [3] it can be computed as

$$\epsilon^{-2}\int_{-D_0(T)}^{D_0(T)}\frac{\partial\varphi_0}{\partial T}+\frac{1}{2}\left(\frac{\partial\varphi_0}{\partial X}\right)^2\,\mathrm{d}X$$

$$=\epsilon^{-2}\left(\frac{D_0^3}{\left(1+D_0^2-T\right)^{\frac{3}{2}}\left(\left(1+D_0^2-T\right)^{\frac{1}{2}}-1\right)}-\frac{1}{2(1-T)^{\frac{1}{2}}}\tan^{-1}\frac{D_0}{(1-T)^{\frac{1}{2}}}\right).$$

Most important for the purposes of this paper is the behaviour of (16) as $T \to 0$. Approximating (16) by

$$\dot{D}_0=\frac{D_0}{D_0^2-T},\quad \text{with}\quad D_0(0)=0,$$

we find that $D_0(T) \sim (3T)^{\frac{1}{2}}$ as $T \to 0$. Hence we have eventually returned to the asymptotic limit as $t \to \infty$ of the Wagner solution, as proposed at the beginning of this section. However, a full justification of the matching between the Wagner and Korobkin regions requires a far more detailed analysis, given in [9, Chapter 3]; suffice it to say that the overlap regime is modelled by a 'large aspect ratio' limit of the Wagner problem or, equivalently, a small-penetration limit of the Korobkin problem (see [2] for a discussion of similar regimes in other codimension-two problems). Our calculation also leads to the interesting prediction of Figure 6. The force on the body increases, initially rapidly (in dimensionless terms, it behaves as $3^{\frac{3}{2}}t^{\frac{1}{2}}$ for small t), then more slowly, until the effect of the base dominates and sends it to infinity like $\frac{1}{2}\epsilon^{-2}(1-T)^{-\frac{1}{2}}$.

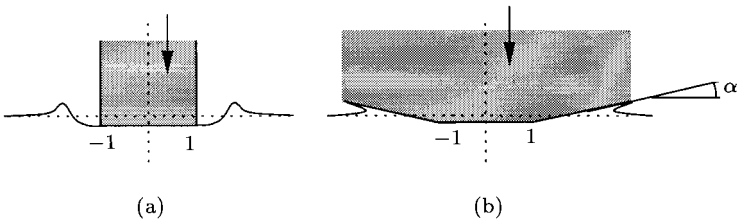

Figure 7. Impact of flat-bottomed bodies.

4. Zero deadrise angle impact

4.1. WAGNER FLOWS

Many generalisations of the theories above suggest themselves, and we focus on just one in this section, namely the case in which the impactor has zero deadrise angle over part of its length and nonzero deadrise angle elsewhere. Thus, in particular, we neglect the cushioning effect of air between the impactor and the water, although it may be expected to be most acute in this configuration; see [11] for a discussion of this topic. Our particular objective here is to investigate how the size of the contact set at $t = 0$ (which was a single point in the models above) affects the slamming mechanics. We only consider infinite-depth slamming in this section, and we scale lengths so that the corners of the body (see Figure 7) are at $x = \pm 1$.

Let us begin by contrasting the flows in Figures 7(a,b). The initial stages of the impact of a rectangle as in Figure 7(a) can be considered as in the text [5, Chapter 6], where it is proposed that for small time the fluid velocity is precisely that predicted by the Wagner theory with the turnover regions fixed at $x = \pm 1$, $y = 0$. This gives the velocity potential

$$\phi(x, y, t) = \mathfrak{Im}\left(-z + (z^2 - 1)^{\frac{1}{2}}\right), \tag{19}$$

where $z = x + \mathrm{i}y$. Hence infinite velocities are again predicted at the two points $x = \pm 1$. In the small deadrise limit $\alpha \to 0$ of Figure 7(b) we could attempt to remove these singularities in the spirit of our analysis of Section 2, but the appropriate initial condition is unclear and we return to this question at the end of this section. When the deadrise angle is not small, and in particular in the configuration of Figure 7(a), the flow near $x = \pm 1$ is even less clear, and we consider this case first, assuming that the deadrise angle α for $x > 1$ is finite and nonzero as $x \downarrow 1$.

In the spirit of the 'wedge entry' problem [1], we might anticipate the existence of a local similarity solution, but this solution may take different forms depending on the size of α and on the assumptions we make as to whether the free surface leaves the body from the corner or from further up the body. For example, if α is large enough, it would be physically reasonable to assume that the free surface leaves from the corner and tangentially to the flat bottom (independently of α) and does not meet the body again. This suggests that the flow is described by a velocity potential which satisfies the free boundary problem shown in Figure 8, in which (x_c, y_c) are now coordinates centred at the corner. The behaviour at infinity is

$$\phi(x_c, y_c, t) \sim \mathfrak{Re}\left(-\mathrm{i}\,(2z_c)^{\frac{1}{2}}\right), \tag{20}$$

while an integration of the kinematic boundary condition shows that the free surface elevation satisfies $\eta(x_c, t) \sim t/(2x_c)^{\frac{1}{2}}$ as $x_c \to \infty$; also $\eta(x_c, 0) = 0$. Note that we do not change to

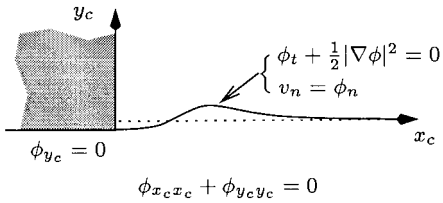

Figure 8. Leading order corner free boundary problem (see the text for the far-field and initial conditions).

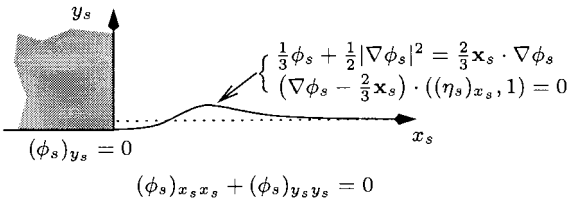

Figure 9. Similarity form of the free boundary problem of Figure 8.

a moving frame as we did in the local analyses of the turnover regions in Sections 2 and 3. This precludes any possibility of a local Helmholtz flow. Also the initial condition is not that $\Phi \equiv 0$ but rather $\phi(x_c, y_c, 0) = \Re e\big(-\mathrm{i}(2z_c)^{\frac{1}{2}}\big)$. Formally a similarity solution is possible [12, 13] in which

$$(x_c, y_c) = t^{-\frac{2}{3}}(x_s, y_s), \quad \phi(x_c, y_c, t) = t^{\frac{1}{3}}\phi_s(x_s, y_s), \quad \eta(x, t) = t^{\frac{2}{3}}\eta_s(x_s). \tag{21}$$

This leads to the free boundary problem shown in Figure 9, in which the far-field behaviour is as in (20), while $\eta_s \sim (2x_s)^{-\frac{1}{2}}$ as $x_s \to \infty$. Near the origin, we have

$$\phi_s \sim c_0 + c_1 x_s + c_2 r_s^{\frac{3}{2}} \sin 3\theta_s/2 + O(r_s^2), \qquad \eta_s \sim a_0 x_s^{\frac{3}{2}} + O(x_s^2),$$

where r_s, θ_s are local polar coordinates and $c_1 > 0$ and c_2 are globally-determined constants, in terms of which

$$c_0 = -3c_1^2/2, \quad a_0 = 4c_2/(15c_1).$$

No other theory is available for this problem but, if it has a solution, the free boundary must have at least one maximum because it is positive for large x_s. Hence if $\eta_s(x)$ has no minima the configuration is as shown in Figure 9. Moreover, fluid is now squeezed out from beneath the impactor, and this generates the maximum shown in the free-surface elevation. By contrast, the jets in Wagner flows comprise fluid from outside the region beneath the impactor.

Even if this similarity solution does exist, it is unlikely that it is the only mathematically possible solution near the corner of the impactor. For example, we could conjecture that surface tension could cause the fluid ejected from beneath the impactor to adhere to its surface near the corner, with separation further up the side, as in the 'teapot' flows of [14], although this may seem unlikely in view of the large velocities at the corner. At any event, the photographs in [7, 13], which appear to show tangential separation and a localised vertical jet some distance from the body, suggest that this does not occur.

Assuming that the scenario sketched in Figure 8 is relevant for large enough α, we now consider what might happen as α decreases. There is a critical angle α_c at which the impactor first touches the free surface and we might conjecture that, for some values of $\alpha < \alpha_c$, there is a similarity solution in which the flow adheres to the impactor for all $x > 1$, or indeed

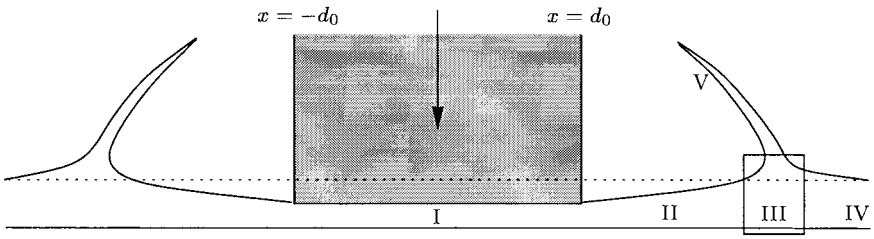

Figure 10. Schematic of zero-deadrise impact in shallow water in the Korobkin flow regime.

separates from the corner and re-attaches further up the body before eventually separating again. We might further suppose that such a flow would be able to be matched with a Wagner flow for which the initial conditions are $\eta(x, 0) = 0$ for $|x| > 1$, $d(0) = 1$, and with initial velocity given by (20). Note that in this scenario, the initial pressure in the Wagner phase is nonzero, being simply given by $-\frac{1}{2}|\nabla\phi|^2$. This reveals another major difference between these flows and those described in Section 2. The fact that, in classical Wagner flows, contact is made instantaneously at only one point means that the initial force on the body is zero; for small t the maximum pressure on the body, at the relative stagnation point in the turnover region, is $O\left((\epsilon^2 t)^{-1}\right)$ while the pressure at the origin is $O\left((\epsilon t^{\frac{1}{2}})^{-1}\right)$.

We finally note the implications of the discussion above for the impact of a slightly blunted wedge with small deadrise angle. Any blunting at all will dramatically affect the solution for sufficiently small time but, if the radius of curvature of the blunted part is of $O(\epsilon^{\frac{2}{3}})$ or greater in our scalings (and this includes the case of a small flat section of lateral extent $O(\epsilon^{\frac{2}{3}})$), the pressure distribution on the impactor will not differ significantly from that on a wedge for times of $O(1)$.

4.2. KOROBKIN FLOWS

Let us now consider basal effects on the scenario described above. For simplicity we only consider the case of rectangular impact and, leaving speculation aside, we assume throughout that the flow separates smoothly from the impactor as in Figure 7(b).

As in Section 2, we use the undisturbed water depth as our length scale, relative to which we define the rectangle breadth to be $2d_0$. When d_0 is $O(1)$ or smaller, the Wagner theory can still be applied in principle while the penetration is of $O(\epsilon)$. We simply replace (19) by (3) with $d(t)$ equal to the constant d_0. We do not pursue this calculation here, but we do remark that when the penetration is of $O(1)$, the numerical solution that would be required to find the surface elevation would be very revealing. The evolution beyond the small penetration regime, with its conjectured associated local 'single hump' morphology as in Figure 9, is an unsolved problem.

There is one other parameter regime where analysis can help, namely when $d_0 \gg 1$; in this situation Korobkin [6] has proposed the following scenario, sketched in Figure 10. By symmetry, we restrict attention to the region $x > 0$. In parallel with the notation of Section 3, we write $x = d_0 X$, and denote time by T (reserving t for time scaled as in Section 2). After an initial transient, the flow is decomposed into five regions. Beneath the impactor, in region I, the usual 'inviscid squeeze film' solution applies, and the analogue of (9) is

$$\frac{\partial \Phi}{\partial X} = \frac{X}{1 - T}.$$

The corresponding pressure is $(1 - X^2)/(1 - T)^2$, which must vanish at $x = 1$ to match with region II. There is now no need to introduce a new region near the exit $X = 1$ as in Section 3, because the pressure remains near zero in region II, even very close to $X = 1$. In region II, which consists of fluid squeezed out from beneath the impactor, the relevant 'zero-gravity shallow-water' solution for $U(X, T)$, $h(X, t)$ must satisfy

$$U(1, t) = \frac{1}{1 - T}, \qquad h(1, T) = 1 - T;$$

hence,

$$U(X, T) = \frac{2 - X}{1 - T}, \qquad h(X, T) = \frac{1 - T}{(2 - X)^2}.$$

This solution cannot, however, extend as far as $X = 2$ because the horizontal jet that it describes collides with the initially quiescent layer in region IV, which we expect to move exponentially slowly as in Section 3. The interaction that occurs is a classical jet-collision problem as described in [15, Chapter 11]. The collision occurs in region III near $X = C(T)$, and creates a jet 'spout' in region V. The condition of zero pressure on either side of this spout gives that

$$\lim_{X \uparrow C(T)} U(X, T) - \dot{C} = \dot{C}, \tag{22}$$

and hence $C(T) = 2 - (1 - T)^{\frac{1}{2}}$. Finally, the spout itself, which is a jet whose thickness is calculated in [6], follows a ballistic path from $\big(C(T), 0\big)$. At time T, the fluid ejected at time τ reaches $\big(C(\tau) + \dot{C}(\tau)(T - \tau), \dot{C}(\tau)(T - \tau)\big)$, and hence the spout centreline is the hyperbola $(2 - X)^2 - y^2 = 1 - T$.

This theory leaves open a major problem concerning the initiation of the flow. For very short times after the initial impact, the motion will, to leading order, be confined to the corner of the impactor as in Figures 8 and 9, basal effects only being important insofar as they determine the global constants that complete the specification of these local solutions. However, for larger times, the penetration will increase enough for the similarity solution of Figure 9 not to apply. It would be interesting to see if there was numerical evidence to show that, as the penetration increases, the maximum in the surface elevation conjectured for the local solution moves out and grows into the spout depicted in Figure 10.

5. Three-dimensional impact

Although the two-dimensional theories discussed above are relatively complete, three-dimensional Wagner and Korobkin flows raise many interesting open questions. In this concluding section we briefly describe those which we consider to be the most interesting, and we present some new solutions. We defer discussion of zero-deadrise impact until the end of the section.

5.1. WAGNER FLOWS

For Wagner flows in which the extent of the equivalent flat plat is no greater than the water depth, the only explicit solutions are for axisymmetric or ellipsoidal impactors on water of infinite depth [16]. Thus numerical approaches, using the variational formulation of [10], are even more attractive. For the purposes of this section, we choose (x, y) as horizontal

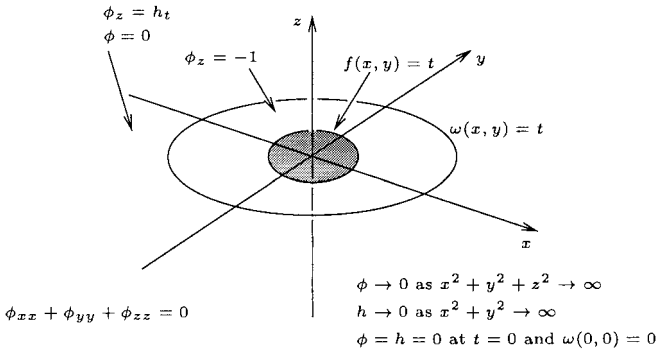

Figure 11. Schematic of three-dimensional Wagner flow.

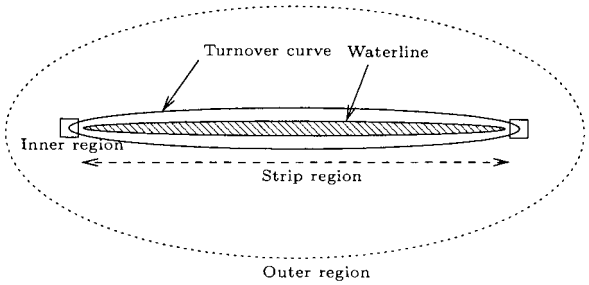

Figure 12. Impact of a slender body.

coordinates, with z vertically upwards. The impactor is $z = \epsilon(f(x, y) - t)$, and the turnover region is now close to a curve which we denote by $t = \omega(x, y)$, $z = 0$. We are especially interested in the relation between the turnover curve and the 'waterline', which we define as the intersection $t = f(x, y)$ of the impactor with the undisturbed free surface $z = 0$. Then the infinite depth Wagner problem is as shown in Figure 11.

Ellipsoidal impact was studied in [16], via the inverse method of specifying the turnover curve in the form $x^2/A^2(t) + y^2/B^2(t) = 1$ and, using ellipsoidal coordinates, looking for an impactor $f(x, y) = x^2/a^2 + y^2/b^2$ for appropriate impactor velocity dependence on t. The calculation is facilitated by knowing the streaming flow past an ellipsoid $x^2/A^2 + y^2/B^2 + z^2/C^2 = 1$ and then letting $C \to 0$, to find a relation between a, b, A, B and t.

However, another interesting limit can be obtained when $a = kb/\epsilon$ ($k = O(1)$) in this solution. We then have the configuration of Figure 12, which is clearly suggestive of the 'strip theory' of slamming. Away from the 'bow' regions, it is easy to show that the lowest order flow in any cross-section $x = \textit{constant}$ is as described in Section 2. Thus, even if the impactor has the general slender shape $z = \epsilon(f(\epsilon x, y) - t)$, the flows in the regions $y = O(1)$, $z = O(1)$ of the planes $x = x_0/\epsilon$ (constant) are independent of each other to lowest order. The 'local slam' starts at time $f(x_0, 0)$ and the local form of the impactor is $z = \epsilon(f(x_0, y) - t)$. Therefore, returning to the impact of the slender elliptic paraboloid, the turnover points in the cross-section $x = x_0/\epsilon$ have y-coordinates $\pm b\,(2(t - f(x_0, 0)))^{\frac{1}{2}}$, *i.e.* the turnover curve has equation $x_0^2/k^2b^2 + y^2/2b^2 = t$.

Near the 'bows' at $x_0 = \pm kb\sqrt{t}$, we have a problem reminiscent of 'leading-edge' problems in aerodynamics. We can scale into an inner region by setting[2] $x - at^{\frac{1}{2}} = \epsilon^2 at^{\frac{1}{2}}\bar{x},\ y = \epsilon^2 at^{\frac{1}{2}}\bar{y},\ z = \epsilon^2 at^{\frac{1}{2}}\bar{z}$ and employ local elliptic paraboloidal coordinates (λ, μ, ν); these are the three roots of $2\bar{x} + \bar{y}^2/(1+s) + \bar{z}^2/s = 1$ and have ranges $\nu \leq -1 \leq \mu \leq 0 \leq \lambda$. Successively fixing λ, μ and ν results in an elliptic paraboloid extending in the negative $\bar{x}$-direction, a hyperbolic paraboloid and an elliptic paraboloid extending in the positive $\bar{x}$-direction. We choose the local turnover curve to be $\lambda = \mu = 0$ (*i.e.* $2\bar{x} + \bar{y}^2 = 1$) so that the local Wagner problem is to find a potential function $\bar{\phi}(\bar{x}, \bar{y}, \bar{z})$ such that

$$\bar{\phi} = 0 \quad \text{on} \quad \lambda = 0, \qquad \frac{\partial \bar{\phi}}{\partial \bar{z}} = 0 \quad \text{on} \quad \mu = 0, \tag{23}$$

the latter condition reflecting the high local velocity that is generated near the turnover region in any Wagner flow. This means that locally the impacting velocity is negligible compared to the induced velocity. We also need to write down the matching conditions with the strip region and the outer region, on the lengthscale of the strip, which drive this local problem. These are easily shown to be

$$\begin{aligned} &\bar{\phi} \sim \sqrt{(1+\lambda)\mu\nu} - \sqrt{\lambda\mu\nu} \quad \text{as} \quad \nu \to \infty, \\ &\bar{\phi} \sim \sqrt{\frac{\mu\nu}{\lambda}} \quad \text{as} \quad \lambda, \nu \to \infty, \quad \text{with} \quad \lambda/\nu = \text{ constant}, \end{aligned} \tag{24}$$

respectively. For the second we have used the fact the leading-order outer flow is driven by a continuous distribution of dipoles on a cut on the x-axis between $x = -at^{\frac{1}{2}}$ and $x = at^{\frac{1}{2}}$; the dipoles have strength and axes determined by matching with strip theory. It is easy to see that the solution of (23) is

$$\phi = ((1+\lambda)\mu\nu)^{\frac{1}{2}} - (\lambda\mu\nu)^{\frac{1}{2}},$$

which provides a description of the flow field near to the pressure maxima where damage is most likely to occur. We expect the inner waterline to be a parabola enclosed by the inner turnover curve $2\bar{x} + \bar{y}^2 = 1$. Indeed, expanding the exact solution of Korobkin [16] reveals that it in fact lies a distance of order $|\log\epsilon|$ away relative to the inner coordinates.

Finally, we remark that our discussion immediately suggests an interesting open question: suppose that the impactor has a ridge line, as in the case of a 'knife-edge' bow. What is the relation between the turnover curve and the waterline? It is possible that a combination of an inverse approach and techniques used in diffraction theory [17] may be able to answer this question.

5.2. KOROBKIN FLOWS

When a body $Z = F(X, Y) - T$ impacts water of unit depth, the large-time model for the flow beneath the impactor, namely (9), generalises to

$$\nabla_{XY} \cdot \Big(\big(1 + F(X,Y) - T\big) \nabla_{XY} \Phi_0 \Big) = 1 \tag{25}$$

[2]For a general smooth body the small inner region has size determined by demanding equal body variation in both the x and y directions.

We denote the lowest order 'turnover curve' in the (X, Y)-plane by $T = \Omega_0(X, Y)$ and assume they are nested and smooth; also Ω_0 vanishes at the initial impact point, and (25) applies in $T > \Omega_0(X, Y)$. Then we can match the flow described by (25) to the nearly static region in $T < \Omega_0(X, Y)$ by locally two-dimensional free-boundary conditions. These conditions are (17), (18) for a parabolic impactor and, more generally, they become

$$\Phi_0 = 0, \qquad \frac{\partial \Phi_0}{\partial N} = 2V_n \left(1 - \frac{1}{(1 + F - T)^{\frac{1}{2}}}\right), \tag{26}$$

on $T = \Omega_0$, where $\partial/\partial N$ denotes the outward normal derivative and V_N is the normal velocity of $T = \Omega_0$. We are thus confronted with an unconventional free boundary problem for Φ_0. One comment that we can make is that the solution, if it exists, can be shown to be stable to small amplitude perturbations under the assumption that the turnover curve expands as time increases. Another is that, for small T, (25) and (26) reduce to

$$\nabla^2_{XY} \Phi_0 = 1$$

with boundary conditions

$$\Phi_0 = 0, \qquad \frac{\partial \Phi_0}{\partial N} = V_N(F - T) \qquad \text{on} \quad \Omega_0.$$

This free boundary problem, which is itself of interest, describes the change in the geometry of the turnover curve as we pass from the Wagner to Korobkin regimes.

6. Conclusion

We have presented a condensed overview of two basic theories of slamming: the 'Wagner theory', in which basal and penetration depth effects are weak, and the 'Korobkin theory', in which they are strong. We have shown that:

1. there are several open questions that need to be answered before these theories can be considered to be complete. Prominent among these are the solution of the free boundary problem of Fig. 8, the initiation of the solution in § 4.2 and the analysis of the new free boundary problems of Section 5.2.
2. reconciliation of the two theories is nontrivial and, in the three-dimensional flow, it leads to the new free boundary problem in Section 5.2.

In a more comprehensive article we could have also discussed three-dimensional zero-deadrise angle impact with strong basal effects. Suffice it to say that an obvious generalization of the model of § 4.2 is the following novel hyperbolic free-boundary problem for the region between the impactor and the spouting water sheet $\partial D(t)$: the velocity potential ϕ satisfies the zero-gravity shallow water equation

$$\frac{\partial \phi}{\partial t} + \frac{1}{2}|\nabla \phi|^2 = \frac{1}{2}|\mathbf{u}|^2,$$

where on the impactor boundary, $\nabla \phi = \mathbf{u}$ is the ejected water velocity and, as in (22), ∂D is determined by

$$\frac{\partial \phi}{\partial n} = 2v_n,$$

v_n being the normal velocity of ∂D.

Finally, we have left open the problem of what happens after the impactor hits the base. Such a study would entail some careful cavitation modelling for the dry region that is revealed by the ejected liquid.

Acknowledgements

We are grateful for helpful comments from A. A. Korobkin. J. M. O. wishes to thank the EPSRC for financial support via a studentship.

References

1. H. Wagner. Über Stoß- und gleitvorgänge an der Oberfläche von Flüssigkeiten (Phenomena associated with impacts and sliding on liquid surfaces). *Zeitschr. Angew. Math. Mech.* 12 (1932) 193–215.
2. S. D. Howison, J. D. Morgan, and J. R. Ockendon. Codimension-two free boundary problems. *SIAM Rev.* 39 (1997) 221–253.
3. A. A. Korobkin. Impact of two bodies one of which is covered by a thin layer of liquid. *J. Fluid Mech.* 300 (1995) 43–58.
4. E. O. Tuck and A. Dixon. Surf-skimmer planning hydrodynamics. *J. Fluid Mech.* 205 (1989) 581–592.
5. G. K. Batchelor. *An Introduction to Fluid Mechanics.* Cambridge: Cambridge University Press (1967) 615 pp.
6. A. A. Korobkin. Shallow-water impact problems. *J. Eng. Math.* 35 (1999) 233–250.
7. A. V. Bukreev and V. I. Gusev. Gravity waves generated by a body falling onto shallow water. *Zh. Prikl. Mekh. Tekh. Fiz.* 37 (1996) 90–98.
8. S. D. Howison, J. R. Ockendon, and S. K. Wilson. Incompressible water-entry problems at small deadrise angle. *J. Fluid Mech.* 222 (1991) 215–230.
9. J. M. Oliver. *Water-Entry and Related Problems.* PhD thesis, Oxford (2002) to appear.
10. A. A. Korobkin. Formulation of penetration problem as a variational in-equality. *Din. Sploshnoi Sredy* 58 (1982) 73–79.
11. F. T. Smith, L. Li, and G.-X. Wu. Air cushioning with a lubrication/inviscid balance. *Preprint* (2001).
12. A. A. Korobkin and V. V. Pukhnachov. Initial stages of water impact. *Ann. Rev. Fluid Mech.* (1988) 159–185.
13. Yu. L. Yakimov. Effect of the atmosphere with the fall of bodies into water. *Izv. Akad. Nauk. SSSR Mekh. Zhidk. Gaza* 5 (1973) 3–6.
14. J. M. Vanden-Broeck and J. B. Keller. Pouring flows with separation. *Phys. Fluids* A(1) (1989) 1456–159.
15. M. L. Milne-Thomson. *Theoretical Hydrodynamics.* Macmillan (1955) 743 pp.
16. Scolan Y.-M. and A. A. Korobkin. Three-dimensional theory of water impact. Part 1. Inverse Wagner problem. *J. Fluid Mech.* 440 (2001) 293–326.
17. L. Kraus and L. M. Levive. *Comm. Pure Appl. Math.* 14 (1961) 49–68.